JOURNAL OF GEOPHYSICAL RESEARCH, VOL. 112, D15111, doi:10.1029/2007JD008394, 2007

Northern Hemisphere annular mode in summer: Its physical significance and its relation to solar activity variations

Jae N. Lee[1] and Sultan Hameed[1]

Received 3 January 2007; revised 26 April 2007; accepted 22 May 2007; published 14 August 2007.

[1] We use the National Centers for Environmental Prediction/National Center for Atmospheric Research reanalysis to calculate empirical orthogonal functions of summer geopotential heights in the Northern Hemisphere at all levels in the troposphere and the stratosphere. The leading patterns in summer are distinct from the patterns in winter. Also, the leading patterns in the summer stratosphere are distinct from the patterns in the summer troposphere. The summer Northern Hemisphere annular mode (NAM) in the stratosphere has the same sign everywhere but shows higher variability at low latitudes unlike the dipolar structure of the winter NAM. A physical interpretation of the summer NAM in the stratosphere is readily apparent because low (high) values of its principal component correspond to warmer (colder) than climatological mean summer conditions in the stratosphere. The summer NAM in the troposphere, on the other hand, is characterized by variability over the Asian monsoon region. Also, the summer NAM in the stratosphere and upper troposphere is correlated with the solar ultraviolet flux, such that in solar maximum conditions the stratospheric circulation is more ''summer-like'' than average and it is less summer-like in solar minimum conditions. The summer NAM is thus seen as a potentially useful tool in investigating the sources of variability in the summer atmosphere.

Citation: Lee, J. N., and S. Hameed (2007), Northern Hemisphere annular mode in summer: Its physical significance and its relation to solar activity variations, *J. Geophys. Res.*, *112*, D15111, doi:10.1029/2007JD008394.

1. Introduction

[2] The Northern Hemisphere annular mode (NAM), defined as the first empirical orthogonal function (EOF) of geopotential height, has been found to be an important tool in the study of variability of the winter hemisphere [*Thompson and Wallace*, 1998, 2000]. The NAM patterns in winter at different heights in the stratosphere and the troposphere are strongly coupled. The pattern in sea level pressure in winter is called the Arctic Oscillation, and it has been shown to be linked to a large number of regional climatic impacts. The vertical coherence of the winter NAM pattern has been useful in investigations of stratosphere-troposphere interactions [*Baldwin and Dunkerton*, 2001] and the influence of solar activity changes on the atmosphere [*Hameed and Lee*, 2005].

[3] In this paper we calculate the NAM in the summer season and discuss its physical interpretation. The annular mode in summer has been previously discussed by *Thompson and Wallace* [2000]. They used geopotential heights for all the months of the year in their EOF calculation and noted that it is dominated by the winter variability. They also pointed out that the annular modes exist in all seasons but the coupling between the tropospheric and stratospheric modes occurs only in winter. They did not display the summer NAM pattern in the stratosphere but noted that it is different from the winter NAM in that its meridional scale is larger. *Ogi et al.* [2004] pointed out that if the NAM is calculated using geopotential height data for all the months and its principal component (PC) regressed with circulation anomalies in different seasons, misleading results for summer may be obtained. This is because the summer season has its own unique leading pattern, which is overshadowed in the pattern obtained from using data for all months of the year. *Ogi et al.* [2004] did the EOF analysis separately for each month using zonally averaged geopotential height fields from 1000 to 200 hPa but in the latitudinal domain from 40°N to the pole, while the calculations of *Thompson and Wallace* [1998, 2000] considered the region 20°N to the pole.

[4] In EOF analysis a different choice of the geographical domain can introduce significant differences in the calculated patterns and their principal components. In this paper we calculate the EOF patterns for the summer season separately for each altitude available in the National Centers for Environmental Prediction/National Center for Atmospheric Research (NCEP/NCAR) reanalysis from 1000 to 10 hPa for the domain 20°N to the pole. It will be seen later that using the extended geographical domain makes an important difference because the Asian monsoon is a key part of the summer variability in the troposphere. Using the pattern at 10 hPa, we show that the summer NAM in the stratosphere has the physical meaning that the low values of its principal component represent an accentuation from the

[1]Institute for Terrestrial and Planetary Atmospheres, State University of New York at Stony Brook, Stony Brook, New York, USA.

0148-0227/07/2007JD008394$09.00

climatological mean summer condition, while the high values correspond to weakening from the climatological summer condition.

[5] The principal component of the leading EOF in July and August at 30 hPa has been calculated by *van Loon and Labitzke* [1998], and they show that it has a decadal variation similar to the solar UV flux for 1975–1995. We investigate this relationship at several levels in the stratosphere and troposphere for the extended period 1948–2004 and find that the strongest relationship with the solar cycle exists at 50 and 70 hPa.

[6] In section 2 we describe our method of calculation, and in section 3 we discuss the structures of the first two EOF modes at 1000 and 10 hPa in summer and compare them with the two leading winter modes. In section 4 we develop a physical interpretation of the leading summer mode in the stratosphere. In section 5 we employ the NAM to investigate the coupling between the solar cycle and stratosphere in the summer. Section 6 considers possible sources of stratospheric variability in summer, and the conclusions are presented in section 7.

2. Methods

[7] We use the NCEP/NCAR reanalysis monthly geopotential height field for 1948–2004 obtained from the National Oceanic and Atmospheric Administration (NOAA) Climate Diagnostics Center (CDC). Climatological mean has been removed at each grid point at a given altitude to calculate the monthly geopotential height anomalies. Data from May to September and from 20°N to 90°N are used to define the summer annular mode at each of the 17 pressure levels ranging from 1000 to 10 hPa. Data are weighted by the square root of cosine of latitude to generate the equal-area weight at each grid point. The first summer mode is defined as the first EOF of the temporal covariance matrix of geopotential height anomalies at each pressure level. Month to month variability of the leading modes of each summer, spanning the 57-year data record, is calculated at each reanalysis pressure level by projecting monthly geopotential height anomalies onto the leading EOF patterns. We thus calculate the EOF for the summer in precisely the same way as for winter as described by *Hameed and Lee* [2005], which is the same method used by *Baldwin and Dunkerton* [2001].

[8] It can be reasonably said that the databases for NCEP/NCAR reanalysis are fewer and of poorer quality for the earlier years. However, *Kistler and Kalnay* [1999] point out that there was a considerable network of rawinsonde stations in the Northern Hemisphere during the late 1940s and early 1950s. We have therefore chosen to present this analysis for the 1948–2004 period. In our comparisons of the summer NAM with the solar cycle the correlations would improve if the period before 1960 is omitted. However, the disagreement in the earlier period is qualitatively not different from that of the later period of 1995–2004. It therefore seems less arbitrary to present the whole record.

3. Structure of the NAM During Winter and Summer

[9] Figure 1a shows the first EOF of geopotential height variance at 1000 hPa during the extended winter from 1948 to 2004. As has been noted by *Thompson and Wallace* [1998], the surface winter NAM (or the Arctic Oscillation) is characterized by cells in polar and subpolar regions, the Azores high region in the Atlantic basin and the Hawaiian high in Pacific basin. We have calculated the corresponding pattern of the Northern Hemisphere summer season from May to September and the first EOF is shown in Figure 1c. We note that the summer pattern is also characterized by a dipole zonal structure like the Arctic Oscillation. The dipole structure of the 1000 hPa summer pattern was also noted by *Ogi et al.* [2004], who did the analysis for the region 40°N poleward. Comparing Figures 1a and 1c, we notice that the main difference is that in the winter mode the highest variability is over the polar region, while in the summer it is over the Asian monsoon region. As seen in Figure 1c, the first summer mode at 1000 hPa describes a zonal circulation around the polar vortex, as in winter, and contains 17% of geopotential height variability.

[10] Figure 1b shows the second EOF pattern for winter. The highest variance in this mode is over the Aleutian low, and it is anticorrelated with the variability over the Icelandic low. Figure 1d shows the second EOF during the summer. One finds that the overall pattern of variability in the second summer mode is similar to the first mode in winter; in the second summer EOF the highest amplitudes are over the Atlantic subpolar region, and a clear signature of the North Atlantic Oscillation is present similar to the first EOF in winter (shown in Figure 1a). Therefore, if the first winter NAM is regressed on the summer geopotential height data to estimate summer variability, the result is likely to be more representative of the second summer EOF than the first summer pattern.

[11] Figure 2 compares the first two EOF patterns for winter and summer at 10 hPa. The first winter pattern (Figure 2a) explains 45% of the variance for the 1948–2004 period, while the corresponding summer pattern explains 73% of the variance. The fact that the first EOF pattern in summer explains such a large fraction of variance is an indication of the simpler character of summer circulation in the stratosphere. While the winter pattern has the highest amplitudes in the polar region and the well-known dipole structure, such that the variability in the subtropical region is of the opposite sign, the summer pattern is characterized by variability of the same sign throughout the Northern Hemisphere, with the highest amplitudes in the tropics and gradually decreasing toward the high latitudes. In Figure 2d the second EOF for summer is shown, and we note that just as at 1000 hPa it has a structure similar to the first winter EOF. It has a more pronounced dipolar contrast between the polar and the tropical regions than in the winter NAM seen in Figure 2a. By contrast, the second winter EOF in Figure 2b emphasizes the opposite modes of variation between the North Atlantic–north Europe and North Pacific regions. The leading EOF patterns at all pressure levels in the stratosphere are generally similar to the 10 hPa patterns shown in Figure 2. Similarly, the leading EOF patterns at the different pressure levels in the troposphere are similar to 1000 hPa patterns shown in Figure 1. However, the patterns in the stratosphere and the troposphere are different from each other, and their principal components are not correlated

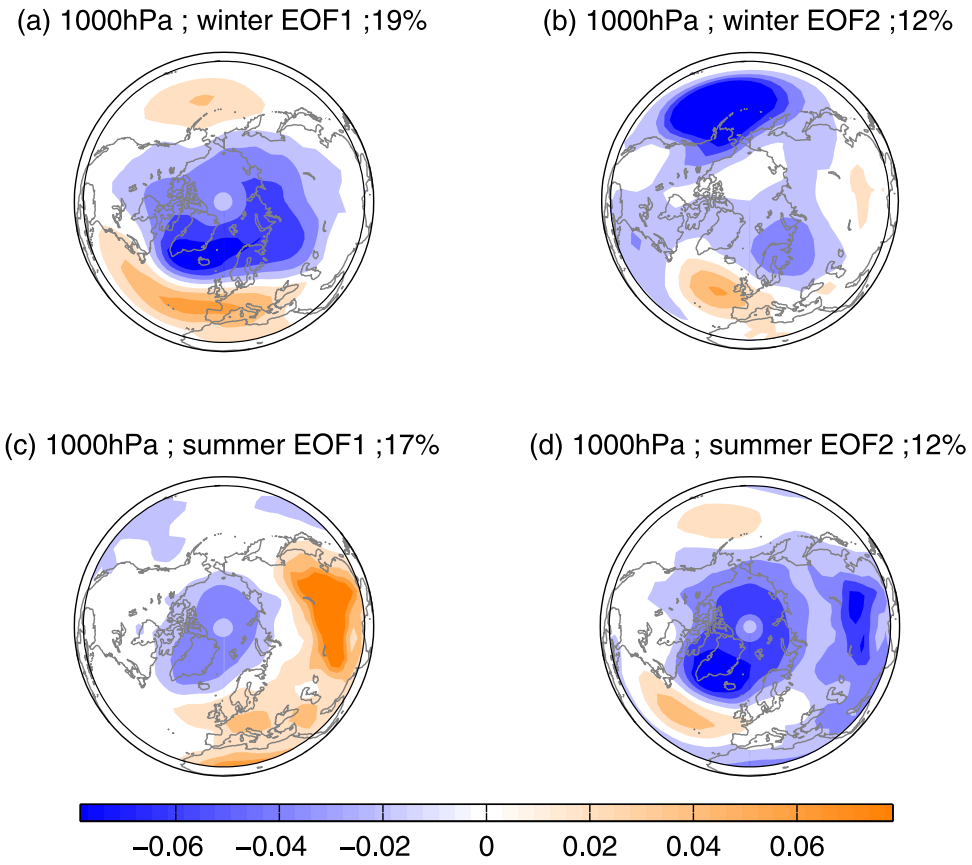

Figure 1. NAM patterns for extended (a and b) winter (from October to April) and (c and d) summer (from May to September) at 1000 hPa. The patterns are calculated as the first and second EOFs of monthly geopotential height for 1948–2004.

during the summer, as was noted by *Thompson and Wallace* [2000].

4. Physical Significance of the Summer NAM

4.1. Stratosphere

[12] We can infer physical significance of the summer NAM patterns by a composite analysis. In section 5 we will see that the relationship between the leading principal component and solar variability is stronger at 50 and 70 hPa. However, the variance contributed by the first mode to the total variance of the geopotential height is greatest at 10 hPa (73%). We therefore explore the physical meaning of the summer NAM at the 10 hPa level. We use it to make two groups of the geopotential height fields. High-NAM index months are defined as those in which the NAM index is above one standard deviation from the mean of the 57 years of summer index values (51 months). Low-NAM index months are similarly defined as those in which the index is below one standard deviation (42 months).

[13] In the climatological mean conditions in summer, there are high temperatures over the arctic stratosphere caused by direct absorption of UV radiation in comparison with lower latitudes. Hence the geopotential heights in the polar regions are high and decrease toward the subtropics giving the geopotential height distribution a dome-like shape centered on the polar region.

[14] As shown in Figure 3, the geopotential height is higher everywhere when the summer NAM index is low in comparison with the high-NAM condition. Moreover, the low NAM is characterized by a larger meridional height gradient. The geopotential height over the polar region is greater by nearly 200 m in low NAM than in high NAM.

[15] In Figure 4 we compare the zonal wind velocities for low- and high-NAM conditions. There is a strong zonally symmetric easterly circulation with very little deformation during the high-NAM periods (Figure 4). The position of the strongest summer easterly jet in the low latitudes is shifted northward during high-NAM periods. However, during low-NAM conditions (Figure 4) the easterly circulation is stronger poleward of about 45°N. The stronger zonal circulation in low-NAM versus high-NAM conditions is consistent with the geopotential height distribution differences in Figure 3.

[16] Figure 5 (left) shows the temperature distribution at 10 hPa in low-NAM conditions, and Figure 5 (right) gives the temperature distribution for the high-NAM composite. We see that the temperature everywhere is colder during high-NAM conditions, especially over the polar region where the temperature difference is 4–6°C between the extremes of NAM. This suggests that the weaker circumpolar circulation during the high-NAM period allows colder air from lower latitudes to mix into the polar regions, resulting in the cold anomalies there and a lowering of the geopotential heights.

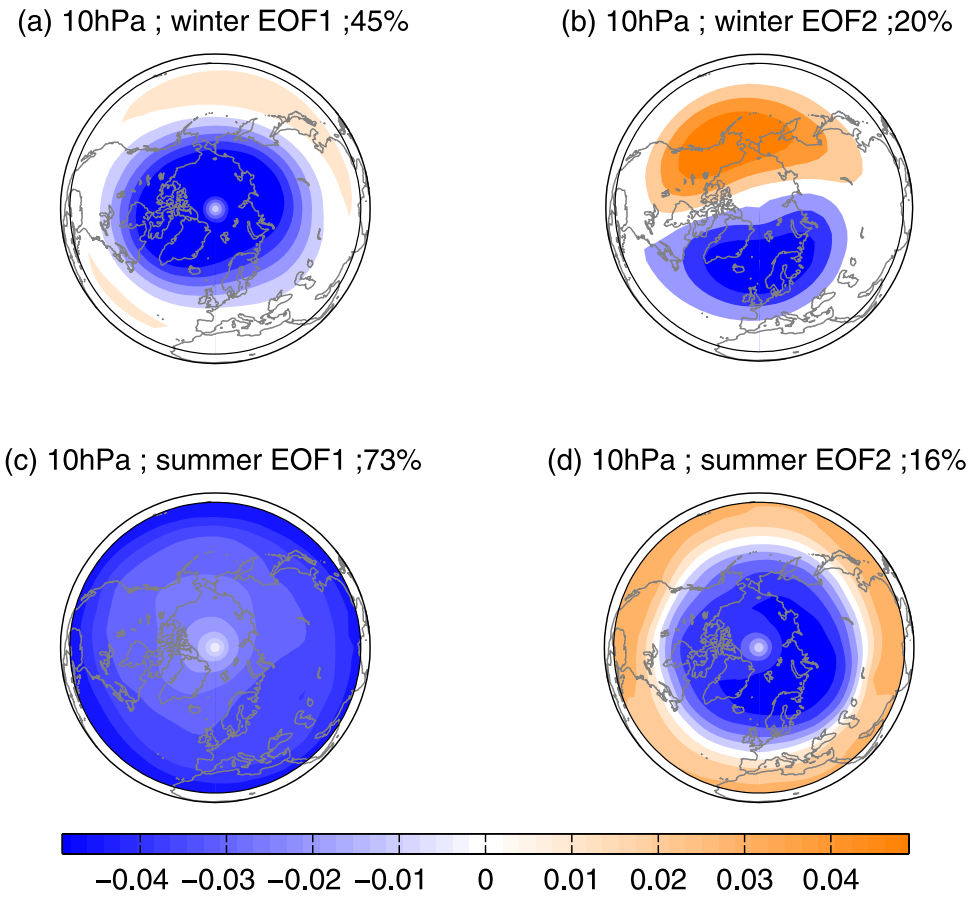

Figure 2. NAM patterns for extended (a and b) winter (from October to April) and (c and d) summer (from May to September) at 10 hPa. The patterns are calculated as the first and second EOFs of monthly geopotential height for 1948–2004.

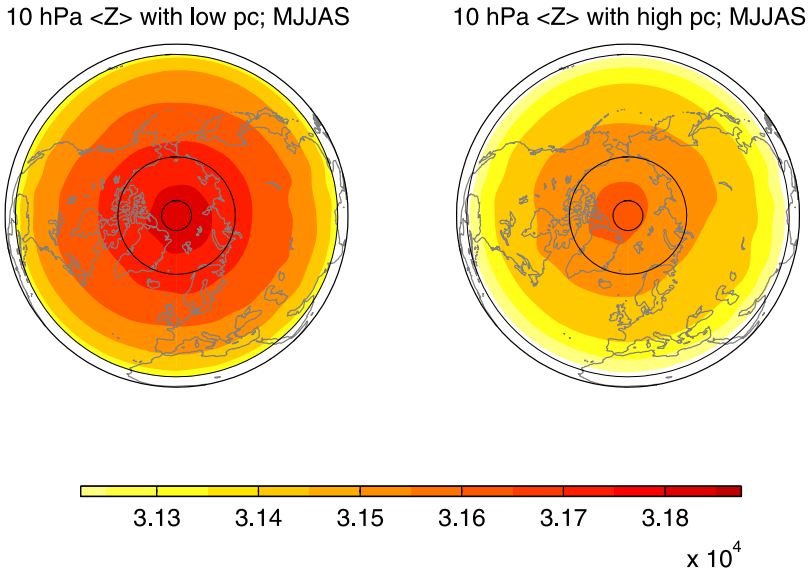

Figure 3. Composites of NCEP geopotential height fields for (left) low-NAM index and (right) high-NAM index at 10 hPa for May–September for1948–2004. The 70°N and 85°N circles are shown for reference. The 20°N latitude is shown as the southern limit of the region being analyzed.

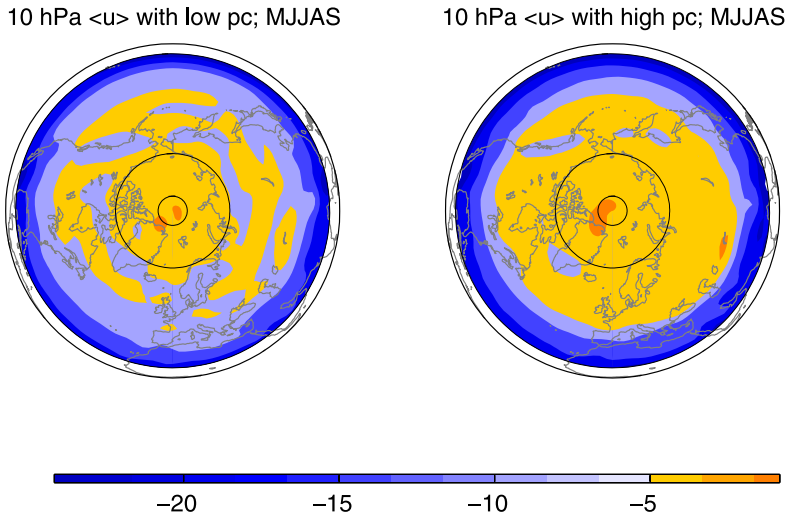

Figure 4. Composite of NCEP zonal wind fields (in m/s) for (left) low-NAM index and (right) high-NAM index at 10 hPa from May to September for 1948–2004. The 70°N and 85°N circles are shown for reference. The 20°N latitude is shown as the southern limit of the region being analyzed.

[17] From Figures 3, 4, and 5 we see that the summer NAM describes the hemisphere-wide variability of the summer stratosphere between conditions, which are more "summer-like" (low NAM) and less summer-like (high NAM). In the less summer-like conditions the temperatures are colder, the easterly zonal circulation is weaker, and the geopotential height distribution is less dome-like than in the climatologically averaged summer condition. In the low-NAM conditions, anomalies opposite to these prevail.

4.2. Troposphere

[18] In Figure 1c, for the leading EOF pattern we see that the largest of variability is over the Asian monsoon region. We did composite analyses for the troposphere using the principal component of the leading pattern at 1000 hPa to define high-NAM index months as those in which it is above 1 standard deviation from the mean of the 57 years. The low-NAM index months are similarly defined as those in which the index is below 1 standard deviation. The composites show that the variability in the Asian monsoon region dominates the variability associated with the leading mode in summer troposphere. As an example, the difference in temperatures in the Northern Hemisphere between low NAM and high NAM in July and August is shown in Figure 6. It is characterized by warmer temperature over the Asian continent and colder temperatures over Siberia. *Greatbatch and Rong* [2006] have shown that spherical Langmuir probes in NCEP/NCAR reanalyses over a region around Mongolia are biased lower than the European Centre for Medium-Range Weather Forecasts re-analysis

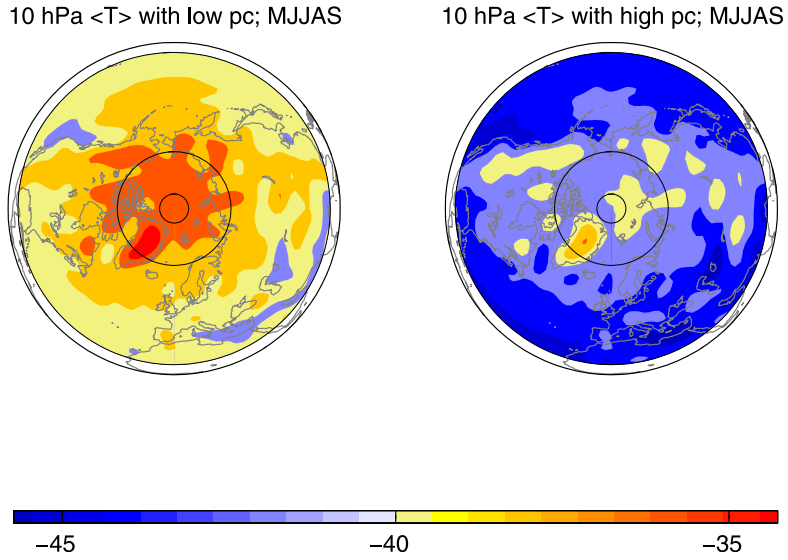

Figure 5. Composite of NCEP air temperature fields for (left) low-NAM index and (right) high-NAM index at 10 hPa from May to September for 1948–2004. The 70°N and 85°N circles are shown for reference. The 20°N latitude is shown as the southern limit of the region being analyzed.

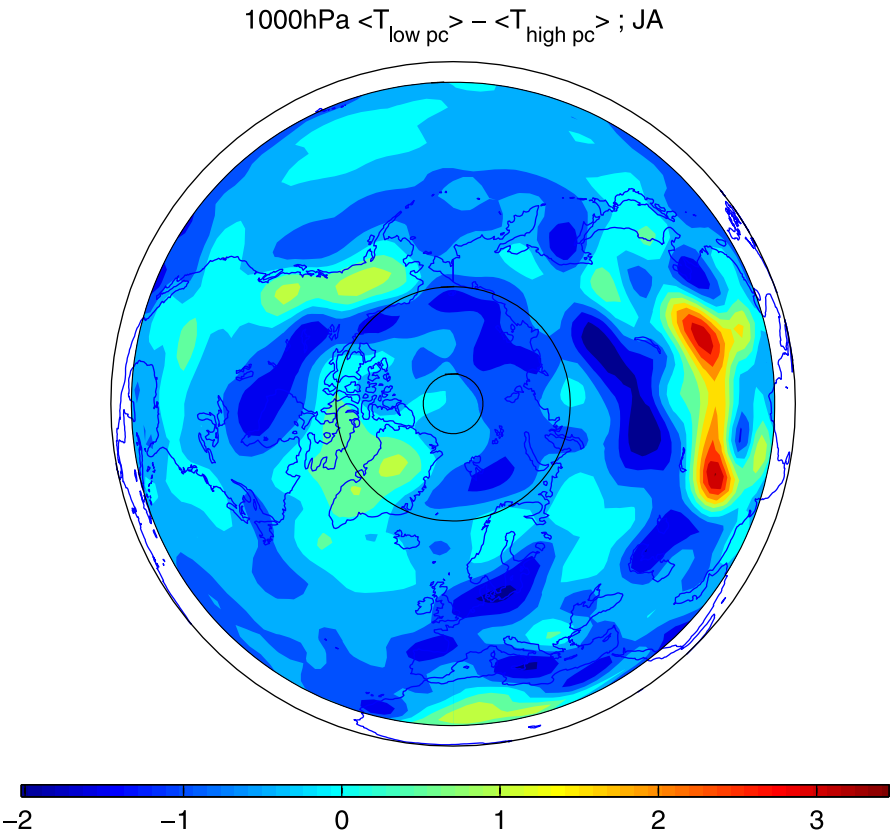

Figure 6. Composite difference of NCEP air temperature fields for low-NAM and high-NAM index at 1000 hPa for July and August for 1948–2004. The 70°N and 85°N circles are shown for reference. The 20°N latitude is shown as the southern limit of the region being analyzed.

(ERA) 40 during 1958–1968. This region is a small part of the positive Asian node in Figure 1c, and it is likely that the pattern may be different in this region if ERA 40 data were used for the analysis.

5. Solar Cycle and the Summer NAM

[19] In their paper, *van Loon and Labitzke* [1998] used NCEP/NCAR geopotential height data averaged for July and August during 1974–1995 and calculated the first EOF at 30 hPa. Their Figure 8 compares the first principal component (PC1) with the 10.7 cm solar flux, and they point out the dominance of the 11-year cycle in both curves. We have extended the analysis to 1948–2004, and the PC1 at 30 hPa is compared with solar UV flux (200–295nm) [*Lean*, 2000] in Figure 7. We note that the agreement between the two curves is weakened after 1995, and it is also less strong in the 1948–1975 period. Nonetheless, the correlation coefficient between the two time series is −0.40. When the autocorrelations in the two series are taken into account using Quenouille's procedure as described by *Angell and Korshover* [1981], the number of independent data points is reduced from 57 to 26. The correlation coefficient is statistically significant at the 95% confidence level for the 1948–2004 periods.

[20] We have repeated this calculation for each month of the extended summer (May–September), separately for the six pressure levels from 10 to 300 hPa, and the results are given in Table 1. Each value gives the correlation coefficient between the principal component of the first EOF for that time period and pressure level with the UV flux (200–295 nm).

[21] Table 1 lists the variance in the May–September geopotential height during 1948–2004 that is explained by the first EOF of the extended summer. The square of the correlation coefficient gives the fraction of the variance in the PC that can be attributed to solar influence. For example, the correlation coefficient for the extended summer at 50 hPa is −0.38, and the variance explained by the PC1 is 58%. Thus about 8% of the geopotential height variance during May–September is attributable to the solar cycle.

[22] In Table 1 we can see that the strongest correlations are in the lower stratosphere, at 50 and 70 hPa, and are during the months of July and August. Since the ozone maximum is also in the lower stratosphere, the results in Table 1 are consistent with the view that the influence of solar variability on the summer stratosphere is primarily via absorption of UV radiation by ozone, which in turn affects the dynamics. Using Total Ozone Mapping Spectrometer (TOMS) ozone data, *Hood* [1997, 2004] has shown that the solar signal is positive and significant with ozone in the lower stratosphere for June, July, and August at low latitudes up to 30°N. *Hood* [1997] estimated that about 85% of the solar cycle variation of global mean total column ozone amount comes from below 30 hPa. Although the results by *Hood* [1997] are for low latitudes

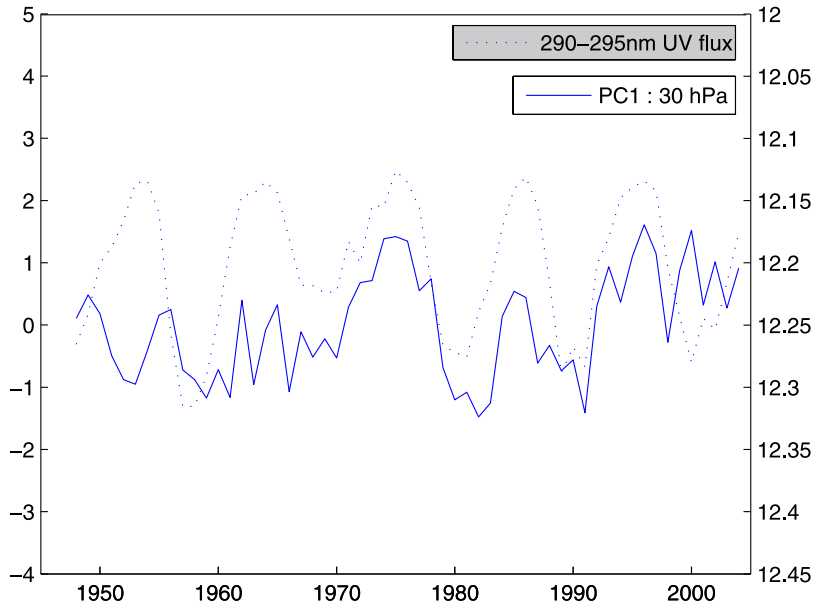

Figure 7. Principal component of the first EOF in the 30 hPa heights in July and August averaged geopotential heights in the Northern Hemisphere with the solar UV flux (200–295 nm). The UV flux scale is inverted.

only, the agreement with the results in Table 1 is encouraging. Of course, the fact that the correlations are highest in the lower stratosphere cannot be taken as proof that the effect is largest there because other simultaneous influences are possible. A global analysis of the satellite ozone data now available would be of much interest in better understanding ozone's role in modulating solar influence on the stratosphere.

[23] The correlations between the UV flux and PC1 are negative; that is, solar maximum (minimum) conditions correspond to lower (higher) summer NAM. This suggests, according to the physical interpretation of summer NAM discussed in section 4, that the stratosphere is more summer-like when the solar cycle is near a maximum. This means that the zonal easterly wind flow is stronger and the temperatures are higher than normal. By contrast, low solar activity corresponds to higher-NAM conditions in which the stratosphere behaves less summer-like. The solar cycle effects therefore appear as small amplitude modulations of the annual cycle, as suggested by *Kodera and Kuroda* [2002].

[24] *Labitzke* [2003] has shown that the geopotential height difference between solar maximum and minimum is greater in the quasi-biennial oscillation (QBO) east phase than in the west phase for the month of July. However, our calculations showed that the correlation between the PC1 and UV flux does not change significantly between the QBO phases during summer. This difference may arise because of our use of the EOFs, which represent hemisphere-wide patterns while the differentiation between east and west phases of the QBO was shown by *Labitzke* [2003] in particular latitude bands.

6. Sources of Variability in the Summer Stratosphere

[25] *Labitzke* [2003] suggested that the effects of solar cycle in the stratosphere may be seen more easily in the summer than in winter because of the low level of variability in the summer season. The NAM explains a greater portion of the geopotential variance in summer than in winter, and the significant anticorrelations of the summer NAM with the solar cycle shown in Table 1 verify *Labitzke*'s [2003] suggestion. Important questions remain, however, about the mechanism of solar UV's interaction with the atmosphere, including the processes that can

Table 1. Correlation Coefficient Between UV Flux and Summer PC1 for 1948–2004[a]

	Variance of PC1 for the Extended Summer	Correlation for the Extended Summer	May	June	July	August	September
10 hPa	73%	−0.26 (28)	−0.19 (24)	−0.21 (23)	−0.32 (24)	−0.36 (27)	−0.22 (27)
30 hPa	68%	−0.34 (32)	−0.33 (33)	−0.30 (31)	**−0.39** (29)	**−0.41** (31)	−0.29 (31)
50 hPa	58%	**−0.38** (35)	**−0.37** 7(41)	**−0.34** (35)	**−0.44** (32)	**−0.44** (33)	−0.29 (30)
70 hPa	47%	**−0.40** (38)	**−0.39** (42)	**−0.36** (36)	**−0.45** (34)	**−0.44** (38)	−0.35 (30)
150 hPa	18%	**−0.35** (40)	**−0.34** (41)	−0.30 (33)	**−0.41** (33)	**−0.37** (37)	−0.31 (30)
300 hPa	8.5%	0.12 (47)	0.00 (43)	0.10 (38)	0.27 (47)	0.18 (49)	0.06 (42)

[a]Bold numbers are correlations with statistical confidence level of 95% or higher. The effective sample size is listed in parentheses in each case.

transfer the solar signal to the lower troposphere. A related topic that merits further investigation is the nature of the variability in the summer stratosphere and its possible sources.

[26] Numerous observational studies have documented traveling and stationary waves in the stratosphere in the summer season. *Muench* [1968], *Randel* [1993], *Miles et al.* [1994], and the studies cited by these authors showed westward propagating Rossby waves in the summer stratosphere in ozone, temperature, and velocity fields.

[27] What processes contribute to the generation of disturbances in the stratosphere? One possible source is the differential heating caused by absorption of UV radiation by the varying concentrations of ozone. Another possibility is the impact of vertically propagating waves from the troposphere.

[28] *Edmon et al.* [1980] and *Wagner and Bowman* [2000] calculated Eliassen-Palm (E-P) flux vectors for summer months in the Northern Hemisphere. Both sets of results show that waves propagate from the troposphere vertically into the stratosphere. A region of flux divergence is seen in the middle-latitude upper troposphere from which wave activity propagates upward. Most of the stratosphere is a region of convergence for E-P flux.

[29] The *Charney and Drazin* [1961] theorem does not rule out planetary waves in the summer. It states that vertical propagation is present when the mean zonal flow $\bar{u}$ relative to phase speed c in the lower stratosphere is westerly but less than a threshold value [*Charney and Drazin*, 1961]:

$$0 < \overline{u} - c < \overline{u_c} \; . \tag{1}$$

This means that traveling waves can propagate vertically into the stratosphere with easterly winds, as long as their westward phase speeds are faster than the zonal mean wind velocity. *Wagner and Bowman* [2000] analyzed daily data for the summer months in the Northern Hemisphere for 1992–1998 and showed that the wave power shifts from eastward propagating waves in the upper troposphere to dominantly westward propagating waves in the middle stratosphere, consistent with the phase speed constraint given by the *Charney and Drazin* [1961] theorem. However, their analysis also showed that the amplitudes of the waves in the summer stratosphere are extremely weak compared to the waves in winter. The sources of summer variability deserve further study.

7. Conclusions

[30] The leading EOF patterns of the summer geopotential heights in the Northern Hemisphere are distinct from the patterns of the winter. Both in the stratosphere and the troposphere the second EOF of the summer geopotential height has structure similar to the first EOF in winter. If the principal components of the leading mode in winter are regressed on summer circulation data, the resulting statistics are likely to represent the second summer EOF pattern. In terms of physical interpretation the low NAM in the stratosphere represents an enhancement of the average summer condition in the geopotential height, temperature, and velocity distributions, and the high NAM is a diminution of the average summer condition. In the troposphere the summer NAM is characterized by the variability of the Asian monsoon; it, however, represents a much smaller fraction off the total variance than in the stratosphere. It was found that the summer NAM in the stratosphere and upper troposphere is inversely correlated with the solar UV flux; that is, in solar maximum conditions the stratospheric circulation is more summer-like than average, and it is less summer-like in solar minimum conditions. The strongest correlations with the solar UV radiation are in the lower stratosphere. Since the EOF patterns in the stratosphere and troposphere are not coupled, a major unanswered question is about the mechanism by which solar cycle induced changes in the summer stratosphere can influence surface climate.

[31] **Acknowledgments.** This work was supported by NASA's Living with a Star Program.

References

Angell, J. K., and J. Korshover (1981), Comparison between sea surface temperature in the equatorial eastern Pacific and United States surface temperature, *J. Appl. Meteorol.*, *20*, 1105–1110.

Baldwin, M. P., and T. J. Dunkerton (2001), Stratospheric harbingers of anomalous weather regimes, *Science*, *294*, 581–584.

Charney, J. G., and P. G. Drazin (1961), Propagating of planetary-scale disturbances from the lower into the upper atmosphere, *J. Geophys. Res.*, *66*, 83–109.

Edmon, H. J., Jr., B. J. Hoskins, and M. E. McIntyre (1980), Eliassen-Palm cross sections for the troposphere, *J. Atmos. Sci.*, *37*, 2600–2616.

Greatbatch, R. J., and P.-P. Rong (2006), Discrepancies between different Northern Hemisphere summer atmospheric data products, *J. Clim.*, *19*, 1261–1273.

Hameed, S., and J. N. Lee (2005), A mechanism for Sun-climate connection, *Geophys. Res. Lett.*, *32*, L23817, doi:10.1029/2005GL024393.

Hood, L. L. (1997), The solar cycle variation of total ozone: Dynamical forcing in the lower stratosphere, *J. Geophys. Res.*, *102*, 1355–1370.

Hood, L. L. (2004), Effects of solar UV variability on the stratosphere, in *Solar Variability and Its Effects on Climate*, *Geophys. Monogr. Ser.*, vol. 141, pp. 283–303, AGU, Washington, D. C.

Kistler, R., and E. Kalnay (1999), The NCEP/NCAR reanalysis prior to 1958, paper presented at Second WCRP International Conference on Reanalyses, Reading, U.K., 2000.

Kodera, K., and Y. Kuroda (2002), Dynamical response to the solar cycle, *J. Geophys. Res.*, *107*(D24), 4749, doi:10.1029/2002JD002224.

Labitzke, K. (2003), The global signal of the 11-year sunspot cycle in the atmosphere: When do we need the QBO?, *Meteorol. Z.*, *12*, 209–216.

Lean, J. (2000), Evolution of the Sun's spectral irradiance since the Maunder Minimum, *Geophys. Res. Lett.*, *27*, 2425–2428.

Miles, T., W. L. Grose, E. E. Remsberg, and G. Lingenfelser (1994), Evolution of the Southern Hemisphere subpolar middle atmosphere during summer and autumn, *J. Atmos. Sci.*, *51*, 677–693.

Muench, H. S. (1968), Large-scale disturbances in the summertime stratosphere, *J. Atmos. Sci.*, *25*, 1108–1115.

Ogi, M., K. Yamazaki, and Y. Tachibana (2004), The summertime annular mode in the Northern Hemisphere and its linkage to the winter mode, *J. Geophys. Res.*, *109*, D20114, doi:10.1029/2004JD004514.

Randel, W. J. (1993), Global normal-mode Rossby waves observed in stratospheric ozone data, *J. Atmos. Sci.*, *50*, 406–420.

Thompson, D. W. J., and J. M. Wallace (1998), The Arctic Oscillation signature in the wintertime geopotential height and temperature fields, *Geophys. Res. Lett.*, *25*, 1297–1300.

Thompson, D. W. J., and J. M. Wallace (2000), Annular modes in the extratropical circulation. part I: Month-to-month variability, *J. Clim.*, *13*, 1000–1016.

van Loon, H., and K. Labitzke (1998), The global range of the stratospheric decadal wave. part I: Its association with the sunspot cycle in summer and in the annual mean, and with the troposphere, *J. Clim.*, *11*, 1529–1537.

Wagner, R. E., and K. P. Bowman (2000), Wavebreaking and mixing in the Northern Hemisphere summer stratosphere, *J. Geophys. Res.*, *105*, 24,799–24,807.

S. Hameed and J. N. Lee, Institute for Terrestrial and Planetary Atmospheres, State University of New York at Stony Brook, Stony Brook, NY 11794-5000, USA.